Available online at www.qu.edu.iq/journalcm
JOURNAL OF AL-QADISIYAH FOR COMPUTER SCIENCE AND MATHEMATICS
ISSN:2521-3504(online) ISSN:2074-0204(print)

Numerical Analysis of Thermal Radiation and Viscous Dissipation Effects on Heat Transfer in a Newtonian Boundary Layer Flow between Porous Plates

Maha Mohammed Ali Thanon[1] , Alaa Abdul Rahim Ahmed[2]

[1] *Department of Mathematics, College Education of Pure Science, Mosul University, Nineveh, Iraq, maha.24esp19@student.uomosul.edu.iq*

[2] *Department of Mathematics, College Education of Pure Science, Mosul University, Nineveh, Iraq, alaahammodat@uomosul.edu.iq*

ARTICLE INFO

Article history:
Received: 09 /02/2026
Rrevised form: 05 /03/2026
Accepted : 08 /03/2026
Available online: 30 /09/2026

Keywords:

Steady state

Thermal radiation

Prandtl number

Rayleigh number

Finite difference technique

ABSTRACT

In the present study, the boundary layer flow of a Newtonian fluid between two parallel porous plates separated by a fixed distance is examined numerically. The influence of viscous dissipation and thermal radiation on the flow field and heat transfer characteristics is specifically considered. The mathematical model of the problem is developed using the governing equations of mass, momentum, and energy for a Newtonian fluid. Suitable nondimensional variables are introduced to convert the governing partial differential equations into coupled ordinary differential equations, which are solved using the finite difference method. A graphical discussion is used to discuss the physical properties of the Reynolds number, Darcy number, Hartmann parameter, Eckert number, Radiation parameter, Rayleigh number and Prandtl number. The variation of a velocity and temperature profiles for various relevant parameters is investigated using graphs.

MSC..

https://doi.org/10.29304/jqcsm.2026.18.22638

1. INTRODUCTION

Boundary layer flow over moving surfaces is an important topic in several industrial and technological fields. Such flows often involve heat transfer processes that reflect the characteristics of non-Newtonian fluids [1]. Nandeppanavar M. M. and Siddalingappa M. N. examined the transport of momentum and heat in a viscous fluid flowing over a nonlinearly stretching surface embedded in a porous medium, taking into account the effects of viscous dissipation and thermal radiation [2]. In their numerical work, Hammadi and Dawood investigated convective heat transfer of water in a semicircular channel with porous boundaries and a closed side, and reported that the flow characteristics are influenced by the channel shape [3]. Khan and his colleagues studied the boundary layer flow and heat transfer of a second-order thin film in a porous medium, paying particular attention to the

∗Corresponding author Maha Mohammed Ali Thanon

Email addresses: maha.24esp19@student.uomosul.edu.iq

Communicated by ‘sub editor’

effects of film thickness and permeability on the cooling and heating behavior over an expandable surface [4]. The flow of a thin nanofluid spray over a stretching cylinder in the presence of a magnetohydrodynamic field was studied, considering heat transfer effects. The effects of the main parameters on velocity and temperature distributions were then analyzed and shown graphically [5]. The study examined unsteady heat transfer of Casson and Williamson nanofluids with graphene nanoparticles flowing over a stretching surface under a transverse magnetic field. It was found that adding graphene improved the thermal conductivity [6]. Bilal et al. studied the heat and mass transfer of a non-Newtonian fluid over an exponentially stretching surface, considering the effects of magnetic fields, chemical reactions, and heat sources [7]. The study by Shehzad et al. examined heat transfer in thixotropic fluids over exponentially stretching surfaces. Similarity transformations were applied to simplify the equations, and numerical results were obtained to show the boundary layer characteristics [8]. Mehta et al. investigated oscillatory flow and heat transfer in a confined porous region between parallel surfaces under an inclined magnetic field, thermal radiation, and a heat source. Analytical solutions were obtained, and the results were presented graphically [9]. Akhtar and Ashraf studied the process of Newtonian fluid flow in a porous medium. This medium is confined between two parallel plates, and they showed how thermal radiation affects the density, thickness, and viscosity of the fluid [10]. Baili et al. studied Oldroyd-B fluid flow over a stretching surface with a magnetic dipole and motile microorganisms, solving the equations numerically and with neural networks [11]. Wang et al. examined heat and mass transfer of a Maxwell nanofluid over a stretching surface, considering solar radiation, chemical reactions, and electromagnetic effects, and found that increasing radiation and reaction rates enhance heat transfer [12]. studied the effect of chemical response at the drift of Maxwell nanofluid by Qureshi et al [13]. Examined the nanolayer impact on the glide of hybrid nanofluids because of the dispersal of nanocomposite material. Cheruku and Reddy [14]. Studied the thermal slip impact at the drift of two fluids in a vertical channel. Furthermore, larger Grashof and molecular Grashof varieties have been shown to be associated with higher angular velocity. Hammodat et al used the finite distinction technique to examine the time-based warmth drift of a vertical plate underneath the influence of thermal radiation and the Lorentz pressure, due to a magnetic area [15]. Abdulsttar and Hammodat handled the trouble of mass and warmth switch in a uniform fluid drift in a porous medium beneath the effect of thermal radiation and magnetic fields [16]. Drawing from the aforementioned studies, this research performs a computational analysis of how thermal radiation and viscous dissipation influence heat transfer mechanisms within a Newtonian boundary layer across a porous medium. It further investigates the velocity and thermal distributions under different physiological factors, with the results shown through detailed graphical illustrations.

2. Problem description and physical configuration:

The research investigates the heat transfer and flow of a viscous, incompressible fluid between two fixed horizontal surfaces separated by a vertical width L. The confining walls are considered to have a porous nature. To describe the flow field, a rectangular coordinate frame is employed, placing the x -axis along the surface of the bottom boundary ($y = 0$), with the y-axis directed vertically. Under the assumption of steady-state conditions, the velocity and temperature profiles are considered one-dimensional, effectively representing the fully developed thermal and flow regimes inside the domain. The fundamental laws of physics governing this system, which include the balance of mass, momentum, and energy, are expressed as:

Mass is conserved by the following equation:

$$\frac{\partial u}{\partial x} + \frac{\partial v}{\partial y} = 0 \qquad \dots (1)$$

The flow dynamics are governed by the following momentum balance equation:

$$\rho\left(u\frac{\partial u}{\partial x} + v\frac{\partial u}{\partial y}\right) = \frac{-\partial P}{\partial x} - \sigma B_0^2 u + \mu\left(\frac{\partial^2 u}{\partial x^2} + \frac{\partial^2 u}{\partial y^2}\right) - \frac{\mu}{K}u \qquad \dots (2)$$

Heat transfer characteristics are expressed via the energy balance:

$$\rho C\mathrm{p}\left(u\frac{\partial T}{\partial x} + v\frac{\partial T}{\partial y}\right) = k\left(\frac{\partial^2 T}{\partial x^2} + \frac{\partial^2 T}{\partial y^2}\right) - \left(\frac{\partial q_0}{\partial x} + \frac{\partial q_0}{\partial y}\right) + \mu\varphi \qquad \dots (3)$$

The viscous dissipation is in the term:

$$\varphi = 2\left(\left(\frac{\partial u}{\partial x}\right)^2 + \left(\frac{\partial v}{\partial y}\right)^2\right) \quad \dots (4)$$

Rosseland approximation [17] is expressed in the form of

$$q_0 = -\frac{4\sigma^*}{3k_0}\frac{\partial T^4}{\partial x} \quad \dots (5)$$

$$q_0 = -\frac{4\sigma^*}{3k_0}\frac{\partial T^4}{\partial y} \quad \dots (6)$$

By applying Taylor series expansion for the termT^4 about the reference temperature T_{w1}we obtain:

$$T^4 = 4TT_{w1}^3 - 3T_{w1}^4 \quad \dots (7)$$

and If we omit the higher-order terms of the expansion, the expression for radiative heat flux in equations (5) and (6) becomes:

$$q_0 = -\frac{16T_{w1}^3\sigma^*}{3k_0}\frac{\partial T}{\partial x} \quad \dots (8)$$

$$q_0 = -\frac{16T_{w1}^3\sigma^*}{3k_0}\frac{\partial T}{\partial y} \quad \dots (9)$$

By taking the partial derivatives of Eq. (8) along the x-direction and Eq. (9) along the y-direction, it follows that:

$$\frac{\partial \mathrm{q_0}}{\partial \mathrm{x}} = -\frac{16\mathrm{T_{w1}^3}\sigma^*}{3\mathrm{k_0}}\frac{\partial^2 \mathrm{T}}{\partial \mathrm{x}^2} \quad \text{and} \quad \frac{\partial \mathrm{q_0}}{\partial \mathrm{y}} = -\frac{16\mathrm{T_{w1}^3}\sigma^*}{3\mathrm{k_0}}\frac{\partial^2 \mathrm{T}}{\partial \mathrm{y}^2} \quad \dots (10)$$

hence, the equation (3):

$$\rho C\mathrm{p}\left(u\frac{\partial T}{\partial x} + v\frac{\partial T}{\partial y}\right) = \left(k + \frac{16T_{w1}^3\sigma^*}{3k_0}\right)\left(\frac{\partial^2 T}{\partial x^2} + \frac{\partial^2 T}{\partial y^2}\right) + 2\mu\left(\left(\frac{\partial u}{\partial x}\right)^2 + \left(\frac{\partial v}{\partial y}\right)^2\right) \quad \dots (11)$$

2.1. Boundary Conditions:

The relevant boundary conditions for this problem are defined as follows:

$$\left.\begin{array}{ll} T(x, y=0) = T_{w1} & T(x, y=L) = T_{w2} \\ u(x=0, y) = v(x=0, y) = 0 & u(x, y=0) = v(x, y=0) = 0 \\ u(x=L, y) = v(x=L, y) = 0 & u(x, y=L) = v(x, y=L) = 0 \end{array}\right\} \quad \dots (12)$$

Where $u, v, P, B_0, \sigma, C\mathrm{p}, K, \rho, T, q_0, \mu, T_{w1}, \varphi, k, k_0, \sigma^*$are pace components in the x, y guidelines, respectively, pressure, consistent magnetic subject, electric-powered conductivity, specific heat at consistent pressure, permeability of medium, density, temperature , radioactive heat flux, viscosity, and preliminary fluid temperature, Viscous dissipative, thermal conductivity, radiation Absorption/Diffusion coefficient, Stefan -Boltzmann consistent respectively.

3. Mathematical Formulation:

After defining the residences and parameters of problem (U_*, L), the variables are used of their non-dimensional form, consistent with the following method. The governing equations are then constructed using those variables, in their non-dimensional form:

$$\left.\begin{array}{lll} x'' = \frac{x}{L}\ , y'' = \frac{y}{L}, & u'' = \frac{u}{U_*}\ , v'' = \frac{v}{U_*}, & P'' = \frac{P}{\rho U_*^2} \\ \vartheta'' = \frac{T - T_{w1}}{T_{w2} - T_{w1}}\ , \quad U_* = \frac{\alpha}{L}\sqrt{RaPr}, & Re = \frac{\rho L U_*}{\mu}, \quad Da = \frac{k}{L^2}, & Ec = \frac{U_*^2}{Cp\Delta T} \\ Ra = \frac{\rho g \beta \Delta T L^3}{\alpha \mu}, \quad Rd = 1 + \frac{16\sigma^* T_{w1}^3}{3k_0 k}\ , & Ha = B_0 L\sqrt{\frac{\sigma}{\mu}}, & Pr = \frac{Cp\mu}{k} \end{array}\right\} \quad \dots (13)$$

Where $Re, Rd,$ Ra, $Pr, Ha,, Ec, Da$ Reynolds number, thermal radiation parameter, Rayleigh number, Prandtl parameter, Hartmann parameter, Eckert number and Darcy number [18]. Hence, the following dimensionless governing equations are obtained:

$$\frac{\partial u''}{\partial x''} + \frac{\partial v''}{\partial y''} = 0 \quad \dots (14)$$

$$u''\frac{\partial u''}{\partial x''} + v''\frac{\partial u''}{\partial y''} = \frac{-\partial P''}{\partial x''} - \frac{(Ha)^2}{Re}u'' + \frac{1}{Re}\left(\frac{\partial^2 u''}{\partial x''^2} + \frac{\partial^2 u''}{\partial y''^2}\right) - \frac{1}{ReDa}u'' \quad \dots (15)$$

$$u''\frac{\partial \vartheta''}{\partial x''} + v''\frac{\partial \vartheta''}{\partial y''} = \frac{Rd}{\sqrt{RaPr}}\left(\frac{\partial^2 \vartheta''}{\partial x''^2} + \frac{\partial^2 \vartheta''}{\partial y''^2}\right) + \frac{2EcPr}{\sqrt{RaPr}}\left(\left(\frac{\partial u''}{\partial x''}\right)^2 + \left(\frac{\partial v''}{\partial y''}\right)^2\right) \quad \dots (16)$$

With the boundary conditions and initial:

$$\left.\begin{array}{ll} \vartheta''(x'', y'' = 0) = 0 & \vartheta''(x'', y'' = 1) = 1 \\ u''(x'' = 0, y'') = v''(x'' = 0, y'') = 0 & u''(x'', y'' = 0) = v''(x'', y'' = 0) = 0 \\ u''(x'' = 1, y'') = v''(x'' = 1, y'') = 0 & u''(x'', y'' = 1) = v''(x'', y'' = 1) = 0 \end{array}\right\} \quad \dots (17)$$

4. Method solution:

The above technique is based on the spiraling way and includes resolving the following equation for one component using repeated variations in steps$\Delta T/2$.Inside the step, every of two stages on this system allows motion for both the x'', andy'' instructions. The first action inside the path of x'' is implied, however the coupling with growing in the role of y'' is made express. In the second stage, the x''-direction motion is stated explicitly, while the y''-direction movement is expressed tacitly. Let's begin with the modern equation. (16), then continue towards the equation (15)[19].

4.1 Solution of Heat Equation:

The x'', and y''instructions have a transfer characteristic that is exactly as follows:

$$u''_{i,j,n}\frac{\vartheta''^*_{i+1,j} - \vartheta''^*_{i-1,j}}{2\Delta x''} + v''_{i,j,n}\frac{\vartheta''_{i,j+1,n} - \vartheta''_{i,j-1,n}}{2\Delta y''} = \frac{Rd}{\sqrt{RaPr}}\left(\frac{\vartheta''^*_{i+1,j} - 2\vartheta''^*_{i,j} + \vartheta''^*_{i-1,j}}{(\Delta x'')^2} + \frac{\vartheta''_{i,j+1,n} - 2\vartheta''_{i,j,n} + \vartheta''_{i,j-1,n}}{(\Delta y'')^2}\right) + \cdots$$

$$\dots + \frac{2EcPr}{\sqrt{RaPr}}\left(\left(\frac{u''^*_{i+1,j} - u''^*_{i-1,j}}{2\Delta x''}\right)^2 + \left(\frac{u''_{i,j+1,n} - u''_{i,j-1,n}}{2\Delta y''}\right)^2\right) \quad \dots (18)$$

$$u''_{i,j,n}\frac{\vartheta''^*_{i+1,j} - \vartheta''^*_{i-1,j}}{2\Delta x''} + v''_{i,j,n}\frac{\vartheta''_{i,j+1,n+1} - \vartheta''_{i,j-1,n+1}}{2\Delta y''} = \cdots$$

$$\dots = \frac{Rd}{\sqrt{RaPr}}\left(\frac{\vartheta''^*_{i+1,j} - 2\vartheta''^*_{i,j} + \vartheta''^*_{i-1,j}}{(\Delta x'')^2} + \frac{\vartheta''_{i,j+1,n+1} - 2\vartheta''_{i,j,n+1} + \vartheta''_{i,j-1,n+1}}{(\Delta y'')^2}\right) + \cdots$$

$$\dots+\frac{2EcPr}{\sqrt{RaPr}}\left(\left(\frac{u''^{*}_{i+1,j}-u''^{*}_{i-1,j}}{2\Delta x''}\right)^2+\left(\frac{u''_{i,j+1,n+1}-u''_{i,j-1,n+1}}{2\Delta y''}\right)^2\right) \quad \dots(19)$$

4.2 Solution of Motion Equation:

$$u''_{i,j,n}\frac{u''^{*}_{i+1,j}-u''^{*}_{i-1,j}}{2\Delta x''}+v''_{i,j,n}\frac{u''_{i,j+1,n}-u''_{i,j-1,n}}{2\Delta y''}=-\frac{P''^{*}_{i+1,j}-P''^{*}_{i-1,j}}{2\Delta x''}+\cdots$$

$$\dots+\frac{1}{Re}\left(\frac{u''^{*}_{i+1,j}-2u''^{*}_{i,j}+u''^{*}_{i-1,j}}{(\Delta x'')^2}+\frac{u''_{i,j+1,n}-2u''_{i,j,n}+u''_{i,j-1,n}}{(\Delta y'')^2}\right)-\left(\frac{1+Da(Ha)^2}{ReDa}\right)u''_{i,j,n} \quad \dots(20)$$

$$u''_{i,j,n}\frac{u''^{*}_{i+1,j}-u''^{*}_{i-1,j}}{2\Delta x''}+v''_{i,j,n}\frac{u''_{i,j+1,n+1}-u''_{i,j-1,n+1}}{2\Delta y''}=-\frac{P''^{*}_{i+1,j}-P''^{*}_{i-1,j}}{2\Delta x''}-\left(\frac{1+Da(Ha)^2}{ReDa}\right)u''_{i,j,n}+\cdots$$

$$\dots+\frac{1}{Re}\left(\frac{u''^{*}_{i+1,j}-2u''^{*}_{i,j}+u''^{*}_{i-1,j}}{(\Delta x'')^2}+\frac{u''_{i,j+1,n+1}-2u''_{i,j,n+1}+u''_{i,j-1,n+1}}{(\Delta y'')^2}\right) \quad \dots(21)$$

5. Graphical Results and Discussion:

In this study, to gain a clear understanding of the physical phenomena, a detailed analysis was conducted to understand the influence of various factors on flow behavior. Specifically, the effects of the radiation coefficient, Reynolds number, Prandtl number, Darcy number, Hartmann number, Eckert number, and Rayleigh coefficient on flow and heat transfer were investigated. These physical effects were clearly demonstrated through the temperature distributions shown in Figures 1-7. In the numerical analysis, a range of values was assigned to each dimensionless coefficient Re, Ha, Ra, Da, Pr, Rd, and Ec to monitor the system's response, and the resulting velocity and temperature profiles were meticulously examined. Specifically, the roles of Re, Da, and Ha were considered. The changes in the velocity fields are presented and discussed in Figures 1, 2, and 3, highlighting their scientific significance in the transfer process. Figure 1 illustrates that as the Reynolds number increases, the fluid velocity also increases. This is due to the relatively low influence of viscous forces compared to inertial forces. At low Reynolds numbers, the flow is largely controlled by viscous forces, which maintains a smooth, layered motion with parallel flow lines and a parabolic velocity distribution. However, as the Reynolds number increases, inertial forces become more significant, propelling the fluid to higher velocities while the viscous shear effect diminishes. This shift results in a marked change in the velocity distribution, which tends to flatten as a large portion of the fluid approaches its maximum velocity near the center of flow. Furthermore, increasing the Darcy number improves the permeability of the porous medium, thereby reducing the frictional resistance within the pores. Consequently, the fluid flows more easily, leading to an increase in velocity, as illustrated in Figure 2. Regarding the magnetic effect, the influence of an external magnetic field on a conducting fluid is determined by the Hartmann number. As the magnetic field becomes stronger, the Hartmann number rises, resulting in the formation of larger electric currents in the fluid. These currents produce a stronger Lorentz force acting against the flow. This magnetic resistance effectively inhibits fluid movement, acting as an additional damping mechanism. Consequently, the flow becomes more turbulent, and the velocity curve becomes more level, while the magnetic effects overcome the internal forces. Therefore, higher Hartmann numbers lead to a significant decrease in fluid velocity, while the role of the magnetic field in stabilizing and slowing down magnetic hydrodynamic flows is reversed, as illustrated in Figure 3.

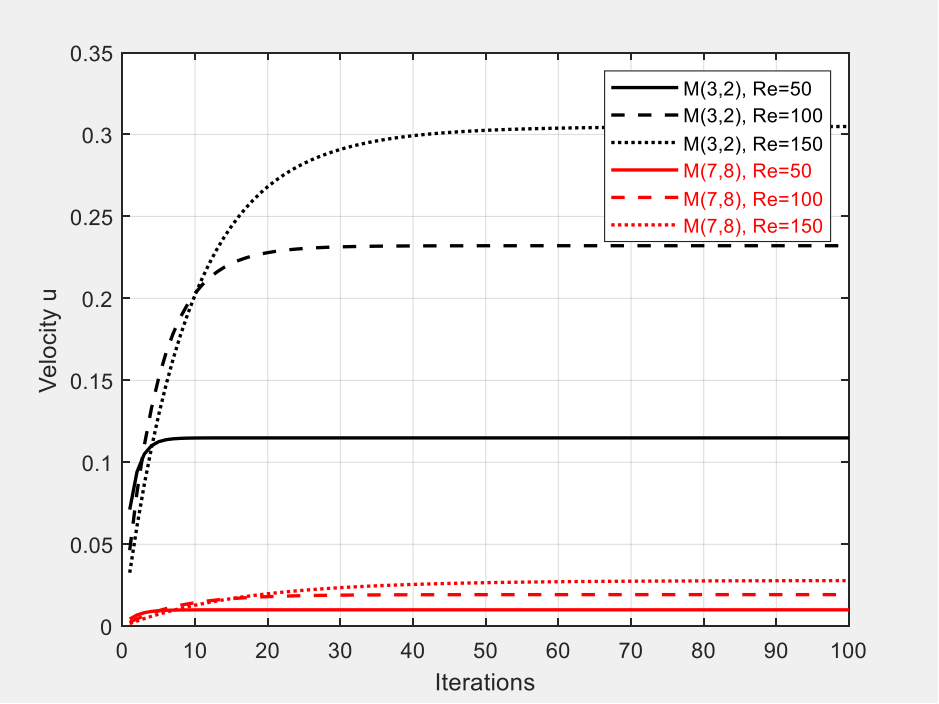

Fig. 1. Variation of the velocity distribution with Reynolds number

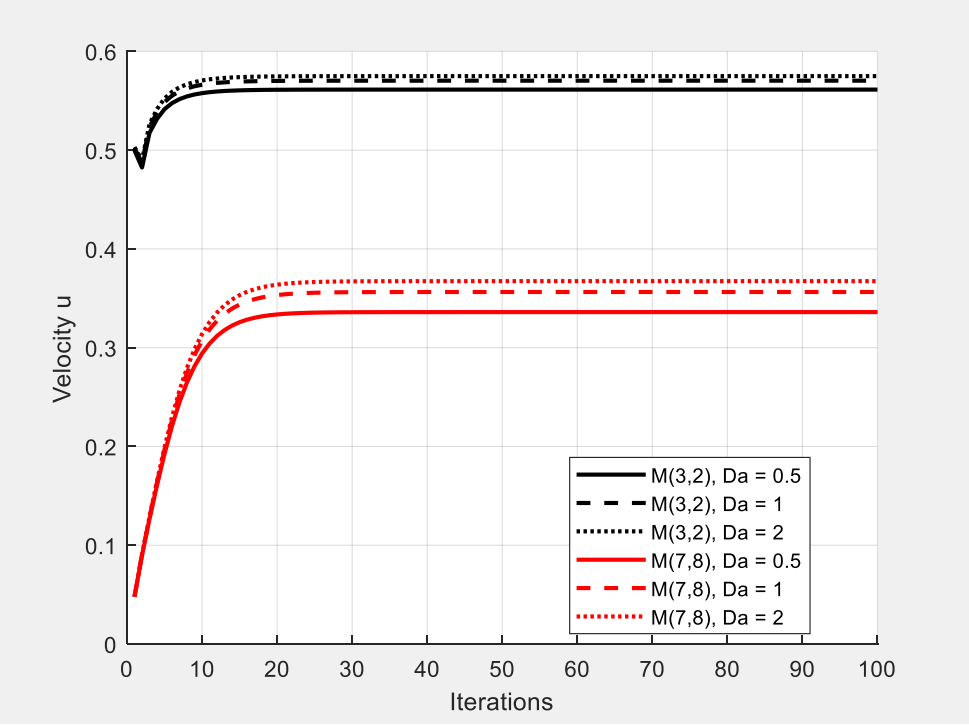

Fig. 2. Variation of velocity profiles against the Darcy number

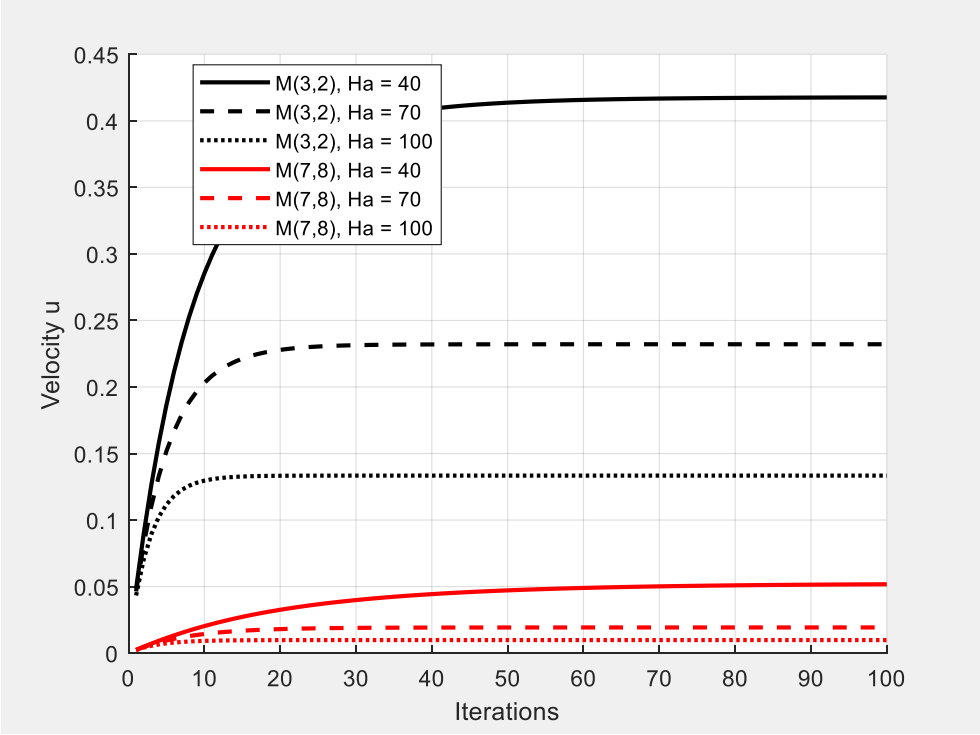

Fig. 3. Variation of velocity profiles with respect to the Hartmann number

The numerical effects show that a growth within the radiation parameter ends in a massive elevation inside the temperature distribution across the float layer. This behavior may be interpreted through the theoretical framework of radiative warmness switch, as this parameter gives a direct degree of the intensity of radiative consequences in the electricity equation. According to the Rosseland diffusion approximation, a boom on this parameter is commonly associated with a reduction within the radiative absorption coefficient of the medium, thereby permitting thermal radiation to propagate greater efficaciously within the fluid. Consequently, a greater quantity of radiative power is absorbed, which enhances inner heating inside the thermal boundary layer Furthermore, the non-dimensional formulation of the electricity equation indicates that the radiative time period capabilities as an additional internal warmness source. An increase in its importance amplifies this supply, resulting in higher non-dimensional temperature values for the duration of the area. The temperature profiles verify that they have an effect on of radiation will become more reported close to the surface, wherein the temperature profiles verify that the temperature gradient decreases, while the thermal boundary-layer thickness will increase. Such physical behavior indicates a decline inside the performance of convective warmness transfer, which is clearly demonstrated as shown in Fig. (4).

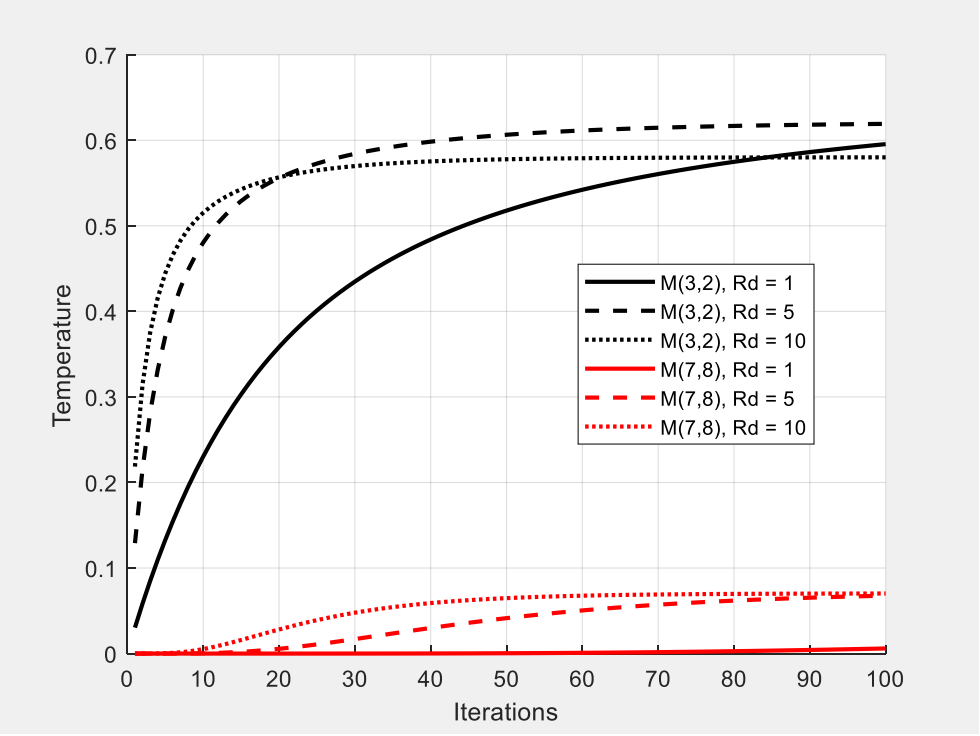

Fig. 4. Variation of temperature profiles with respect to the radiation parameter

As illustrated in Figures 5 and 6, the fluid temperature within the flow layer rises notably as both Rayleigh (Ra) and Prandtl (Pr) numbers grow. This phenomenon aligns with the fundamental concepts of convectional heat transfer. Rayleigh's number reflects the intensity of natural convection resulting from thermal buoyancy. Therefore, a higher Rayleigh's number corresponds to increased fluid movement and a greater heat transfer process due to buoyancy. Accordingly, a substantial quantity of heat is conducted from the hot surface to the nearby fluid layers, which elevates the overall temperature distribution across the entire region. An increase in significantly lowers thermal diffusivity in terms of the Prandtl variety, which measures the ratio of momentum diffusivity to thermal diffusivity. The fluid's ability to transfer heat away from the surface is limited by this reduction. Longer nearby temperatures will result from a thinner thermal boundary layer and improved heat retention near the surface. The blended impact of higher Ra and Pr amplifies inner heating within the fluid, elevating the overall temperature across the float layer. After that, the temperature gradient decreases and the thickness of the thermal boundary layer increases. These patterns are consistent with physiological expectations and support results found in the literature on convective heat transfer in low-thermal diffusivity fluids.

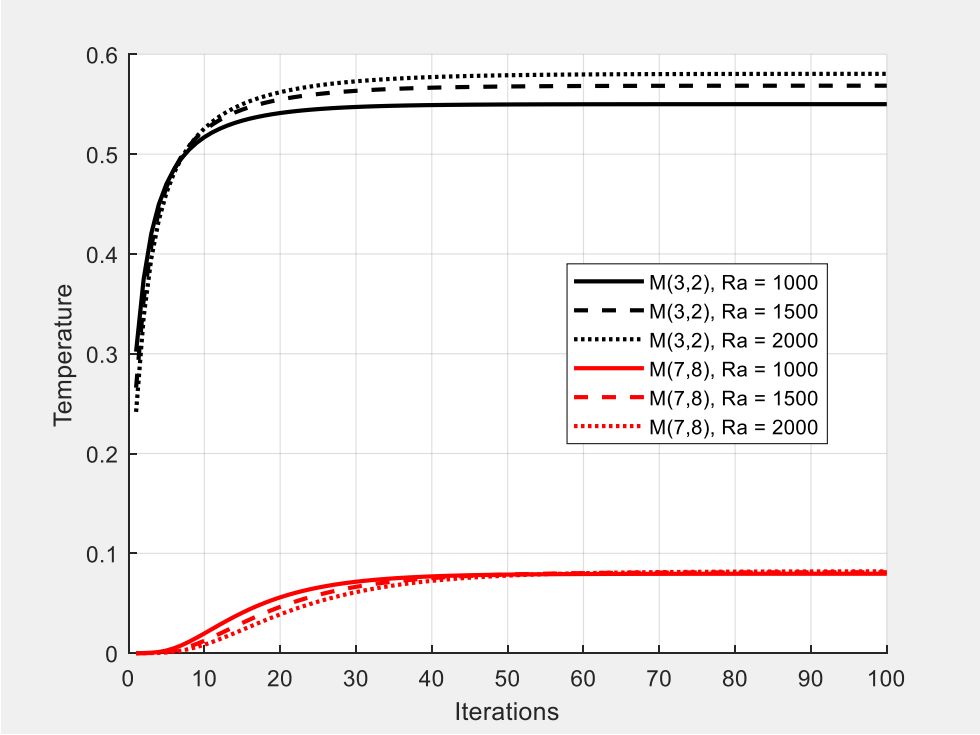

Fig.5. Thermal field response across computing iterations for diverse Rayleigh (Ra) values

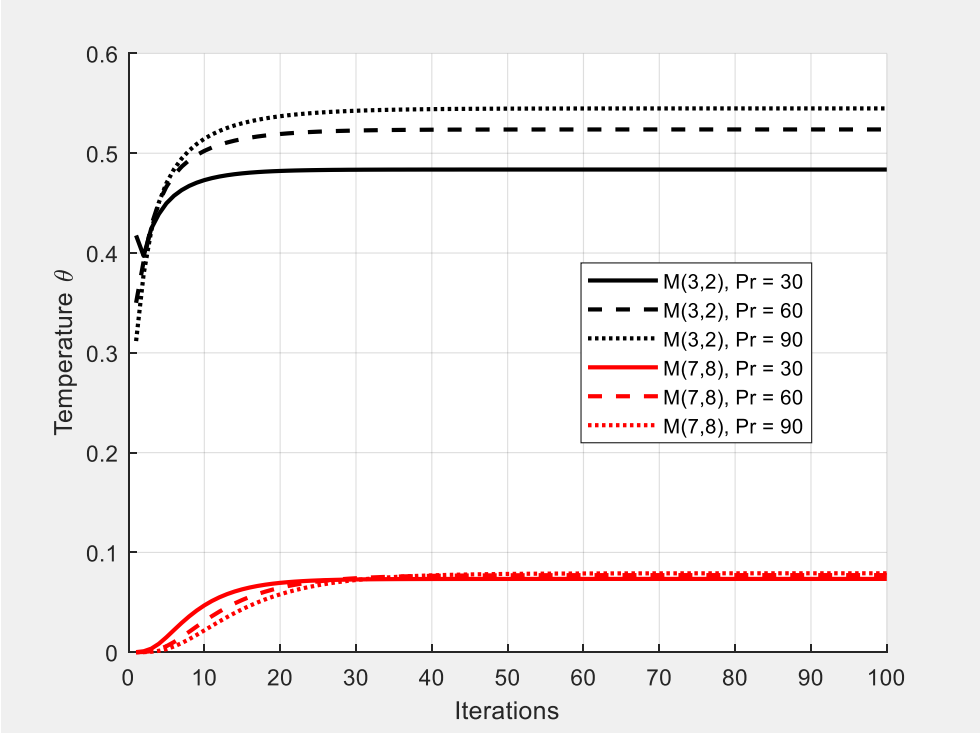

Fig.6.Temperature distribution for various values of Prandtl number

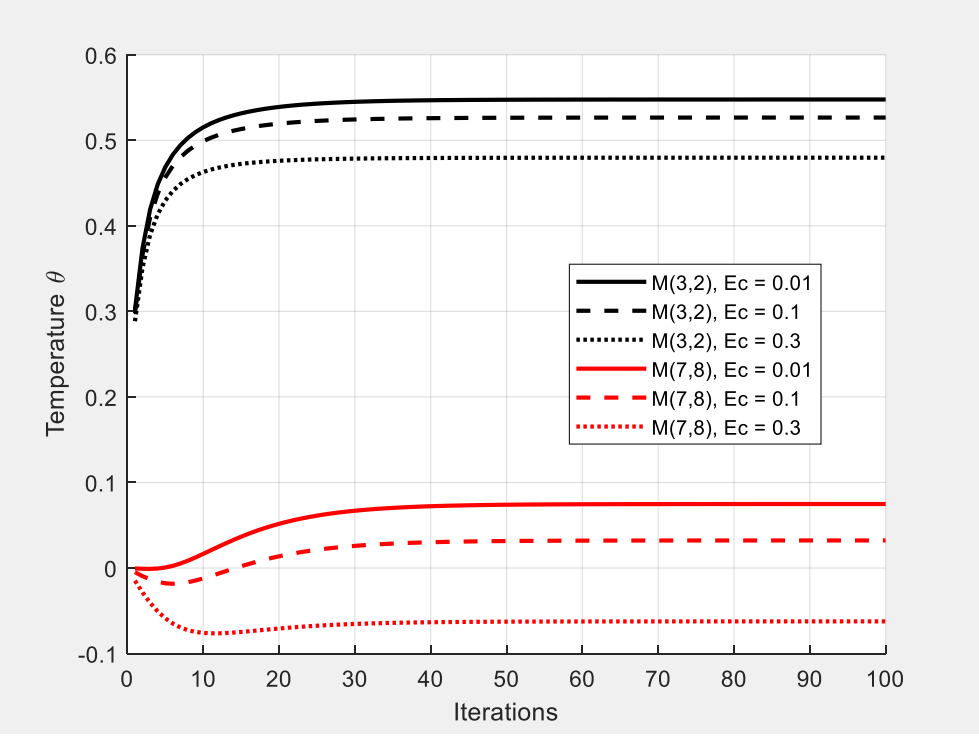

Fig.7. Impact of Ec on profile of temperature

Finally, It is observed that increasing the Eckert number accelerates the convergence toward steady-state conditions. Physically, a higher Ec enhances viscous dissipation, which converts kinetic energy into internal thermal energy. This internal heat generation strengthens thermal damping within the boundary layer, thereby reducing transient fluctuations and promoting faster stabilization of the temperature field as shown in fig. (7).

6.Conclusions:

The outcomes of thermal radiation and viscous dissipation on warmth switch in a Newtonian boundary layer waft had been numerically analyzed in this study. The effects for speed and temperature are acquired and plotted graphically. The principal conclusions of this take a look at are as follows:
(1) Velocity will increase with growing Re and Da, while it decreases with growing values of Ha.
(2) As Ec increases, the temperature decreases; as $Rd, Ra,$ and Pr do, it increases.

References

[1] Remus D.E., Nicolina P., and Rodica B. Heat and mass transfer analysis for the viscous fluid flow dual approximate solutions. Mathematics 2023, 11, 1648.
[2] Nandeppanavar M.M, and Siddalingappa M.N. Effect of viscous dissipation and thermal radiation over a non-linearly stretching sheet through porous medium, Int. J. of Applied Mechanics and Engineering, 2013, vol.18, No.2, pp.461-474.
[3] Hammadi, M. A., & Dawood, A. S. Numerical analysis of fluid flow and heat transfer by forced convection in channel with one-sided semicircular sections and filled with porous media. Journal of Engineering, 2015, 21(05), , pp.1-21.
[4] Khan, N.S. Islam, S., Gul, T., Khan, I., Khan, W., Ali, L. Thin film flow of a second-grade fluid in a porous medium past a stretching sheet with heat transfer. Alex. Eng. J. 2018, 57, 1019–1031.
[5] Khan, N.S., Gul, T., Islam, S., Khan, I., Alqahtani, A.M., Alshomrani, A.S. Magneto hydrodynamic Nano-liquid thin film sprayed on a stretching cylinder with heat transfer. Appl. Sci. 2017, 7, 271.
[6] Zuhra, S., Khan, N.S., Khan, M.A., Islam, S., Khan, W., Bonyah, E. Flow and heat transfer in water based liquid film fluids dispensed with grapheme nanoparticles. Results Phys. 2018, 8, pp.1143–1157.
[7] Bilal, A.M., Alsaedi, A., Hayat, T., Shehzad, S.A. Convective Heat and Mass Transfer in Three-Dimensional Mixed Convection Flow of Viscoelastic Fluid in Presence of Chemical Reaction and Heat Source/Sink. Comp. Math. Math. Phys. 2017, 57, pp.1066–1079.
[8] Shehzad, S.A., Hayat, T., Alsaedi, A. Flow of a thixotropic fluid over an exponentially stretching sheet with heat transfer. J. Appl. Mech. Tech. Phys. 2016, 57, pp. 672–680.

[9] Mehta, T., Mehta, R., & Mehta, A. Oscillatory fluid flow and heat transfer through porous medium between parallel plates with inclined magnetic field, radiative heat flux and heat source. International Journal of Applied Mechanics and Engineering, 2020, 25(2), pp. 88-102.
[10] Akhter, S., & Ashraf, M. Numerical study of flow and heat transfer in a porous medium between two stretchable disks using quasi-linearization method. Thermal Science, 25(2 Part A), 2021, pp. 989-1000.
[11] Baili, J., M J, R. N. K., et al. Multilayer neural networks for studying three-dimensional flow of non-Newtonian fluid flow with the impact of magnetic dipole and gyrotactic microorganisms. *Physica Scripta*, 2023, 98(11), 115228. https://doi.org/10.1088/1402-4896/acfe5e
[12] Wang F, Jamshed W, Usman, et al. Solar radiative and chemical reactive influences on electromagnetic Maxwell nanofluid flow in buongiorno model. J Magn Mater. 2023; 576:170748. doi: 10.1016/j.jmmm.2023.170748
[13] Qureshi MZA, Faisal M, Raza Q, et al. Morphological nanolayer impact on hybrid nanofluids flow due to dispersion of polymer/CNT matrix nanocomposite material. AIMS Math. 2023;8(1):633–656. doi: 10.3934/math.2023030.
[14] Cheruku V, Reddy BR. Numerical study in effect of thermal slip on two fluid flow in a vertical channel. Transactions on Energy Sys and Engineering Appl. 2023;4(2):1–18. doi: 10.32397/tesea.vol4.n2.517
[15] Hammodat, A. A., Al-Obaidi, I., &Algwauish, G. M. A Study of unstable MHD free convection over a vertical plate in two dimensions under the influence of radiation. Al-Qadisiyah Journal of Pure Science, 2024, 29(2), 20.
[16] Abdulsattar, A. A., &Hammodat, A. A. Flow and heat transfer between two parallel surfaces in a porous medium under the influence of a magnetic field and a radiant heat source. In AIP Conference Proceedings, 2025, 3282,1, p. 050070). AIP Publishing LLC.
[17] Cogley, A. C., Vincent, W. G., & Gilles, S. E. Differential approximation for radiative transfer in a nongrey gas near equilibrium. Aliaa Journal, 1968, 6(3), pp. 551-553.
[18] Hammodat A. A., and Dawood H. Numerical solution of electromagnetic problem in horizontal porous medium, ITALIAN JOURNAL OF PURE AND APPLIED MATHEMATICS – N. 47–2022 (1118–1135).
[19] Wilson H.B., and et al. Advanced Mathematics and Mechanics Applications using MATLAB 3rd Ed., Chapman and Hall/CRC, USA.2003.